

THE DESIGN OF THE END MAGNETS FOR THE THIRD STAGE OF MAMI

H. Herminghaus, U. Ludwig-Mertin \*)  
 Institut für Kernphysik, Johannes-Gutenberg Universität Mainz,  
 Johann-Joachim-Becher Weg 33, 6500 Mainz

Introduction

The third stage of the c.w. electron accelerator MAMI (Mainz Microtron)<sup>1,2,3</sup> (fig. 1) will have an output energy of 846 MeV. This will be achieved in 74 turns with an input energy of 180 MeV. This acceleration of 9 MeV/turn corresponds to a magnetic field of 1.5412 Tesla in the end magnets. Because of saturation of the iron the yokes should have the same field density. Therefore the area of the yokes has to be the same as the area of the pole pieces.

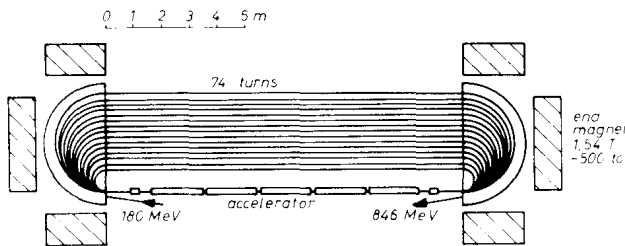


Fig. 1: Scaled scheme of the 3rd stage of MAMI

In order to save iron a configuration with a semicircular pole piece and a half cylindrical yoke would be the best. In case of the microtron magnets, however, a good access through the yoke to the vacuum chamber and a possibility to install a field control is necessary. Therefore a H-C-magnet configuration as shown in fig. 2 should be the best compromise with respect to the iron weight<sup>4</sup>.

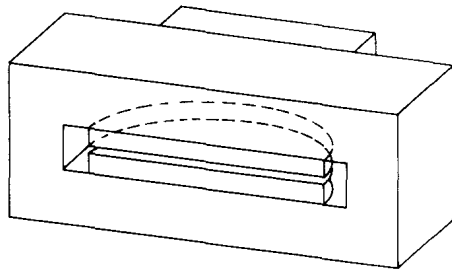


Fig. 2: Scheme of the H-C-configuration for the end magnets of the 3rd stage of MAMI

For beam optical reasons a good homogeneity over a large region of the pole pieces is required.

For the design of those magnets numerical field computations are necessary.

Programs Used for Field Calculations

Three-dimensional field calculations were done by W. Müller and coworkers at the Technische Hochschule Darmstadt by their program PROFI<sup>5</sup> (program for field calculations). This program uses a rectangular grid to describe the magnet geometry. It solves the Maxwell-equations by the method of finite differences.

\*) Work supported in part by Deutsche Forschungsgemeinschaft.

Some model calculations, the design of the reverse field stripe (for vertical focusing) and the inactive clamp were done by the two-dimensional program POISSON<sup>6</sup> at GSI which uses a nonuniform triangular mesh to solve the Poisson's equation by a successive point over-relaxation method.

Results of Three-Dimensional Field Calculations

Fig. 3 shows the geometry of one half of the symmetrical H-C-magnet and the field distribution calculated by PROFI. The distance between the lines of constant field is  $1 \cdot 10^{-3}$ . Large field gradients can be seen especially near the edges of the pole pieces. The field decrease over the region seen by the beam is 2.5 %. The largest gradient near the corners of the poles is about  $6 \cdot 10^{-4}$ /cm. This gradient cannot be corrected by the surface coils successfully used for the first<sup>2</sup> and second<sup>7</sup> microtron of MAMI. Therefore additional shimming will be necessary.

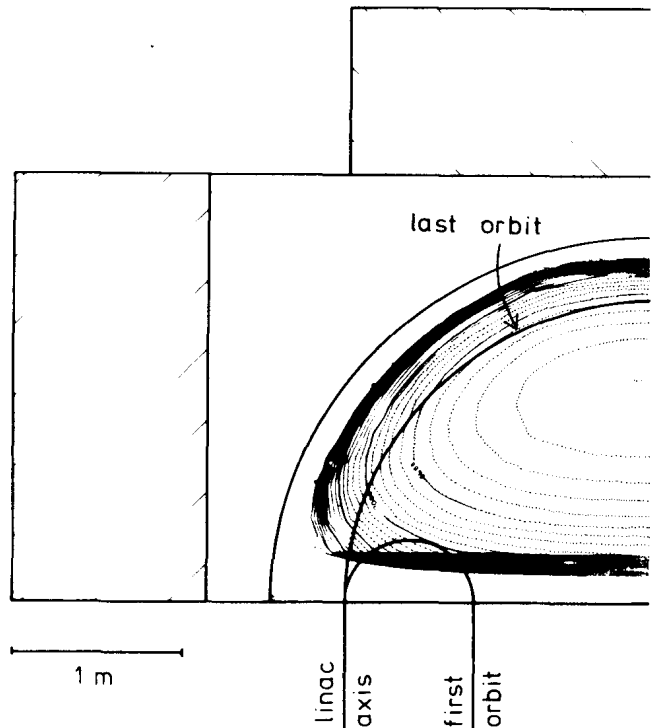


Fig. 3: One half of the H-C-magnet with the field map computed by PROFI (distance between the lines of constant field  $1 \cdot 10^{-3}$ )

The distance between the pole pieces for this calculation was 12 cm. New considerations showed that 10 cm will be sufficient for the vacuum chamber and field corrections. However, the calculation shows nearly the same field gradients for the reduced gap.

Fig. 4 shows a H-magnet configuration. In this case the area of the yoke is obtained by enlarging the back parts of the side yokes. These yokes will be made by separate iron profiles formed like an "U". For

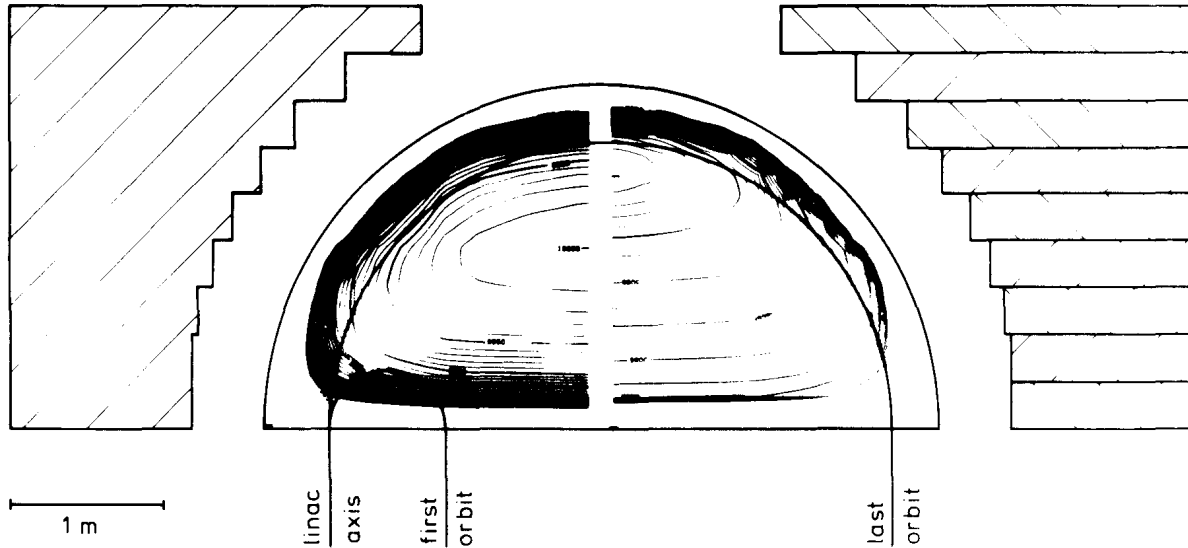


Fig. 4: Geometry of the H-magnet and field map calculated by PROFIT: left half without gaps, right half with gaps between the yoke profiles

lowering of costs the surfaces between the yoke parts should be roughly machined only. Hence there are gaps of about 5 mm between the yoke profiles.

Fig. 4 shows the calculated field map without (left part of the map) and with (right part of the map) consideration of the influence of these gaps. For the numerical calculation with PROFIT the gaps were taken into consideration by reducing the permeability of the iron in direction perpendicular to the entrance pole edge. In case of the isotropic permeability the field gradients are nearly the same as in the H-C-configuration. If the gaps are taken into consideration the field maximum is no more in the midth of the magnet. It is shifted to the round end of the pole piece. This means that the gradient over the whole region seen by the beam is now of about 3 % but the largest gradient to be corrected will be the same as for the H-C-configuration.

Originally the pole pieces were planned to form separate parts which are separated from the yokes by a Purcellgap. An evaluation of the forces calculated from the field distribution given by PROFIT showed that the pole pieces will be pulled by 80 kN in direction to the reverse field stripe situated in front of the magnet, giving important problems for the fastening of the pole pieces. Therefore they should be integrated to the yokes. In this case there will be one or more gaps parallel to the entrance pole edge through the whole pole piece because the weight of each iron block is limited to 80 to (capacity of the crane). A PROFIT calculation shows that the influence of a gap of 0.3 mm is negligible for the field distribution in the midplane.

Field Correction by Shimming

Theory

For shimming the following procedure can be applied: The field gradients (fig. 3,4) are the result of the angle of the magnetic field lines to the pole surface. Therefore the pole has to be rotated in such a way that the lines are perpendicular to the midplane

(fig. 5). For the transition of the field from iron to air the following law of refraction is valid

$$\operatorname{tg} \alpha = \mu \operatorname{tg} \beta.$$

Thus, in a first approximation, the pole surface has to be rotated by an angle  $\delta$  and  $\alpha$  is changed to  $\alpha + \delta$ . The law of refraction is now

$$\operatorname{tg}(\alpha + \delta) = \mu \operatorname{tg} \delta.$$

If  $\delta \ll 1$  it is given by

$$\delta = \frac{\operatorname{tg} \alpha}{(\mu - 1)} \quad (1)$$

In numerical field calculations the field components in the iron near the boundary are known and the angle  $\delta$  of the pole rotation can be calculated.

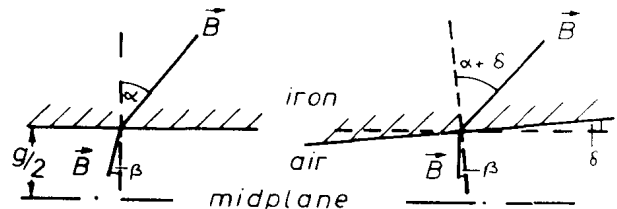


Fig. 5: Shimming by rotating the pole piece in such a way that the field line is perpendicular to the midplane

In case of a measured field only the field component perpendicular to the midplane in the air is known. Therefore another method for the determination of  $\delta$  is required. From  $\operatorname{rot} \vec{B} = 0$  follows

$$\frac{\partial B_y}{\partial x} = \frac{\partial B_x}{\partial y}$$

Assuming that the field gradient is approximately linear

$$\frac{\partial B_x}{\partial y} = \frac{B_x}{g/2}$$

one gets

$$B_x = \frac{g}{2} \frac{\partial B_y}{\partial x}$$

Now the angle of the field lines in the air at the boundary is given by

$$\text{tg} \beta = \frac{B_x}{B_y} = \frac{g}{2} \frac{\Delta B/B}{\Delta x} \quad (2)$$

In consideration of the change of  $\alpha$  to  $\alpha + \delta$  one gets

$$\text{tg} \delta = \frac{\mu}{(\mu-1)} \text{tg} \beta$$

This can be neglected because the influence is less than 1 % for  $B = 1.54$  Tesla.

By this method the angle of the pole rotation necessary for the field correction can be calculated from a field map measured at the upper or lower pole piece.

Results of Two-Dimensional POISSON Calculations

The two-dimensional calculations by POISSON show not so large field gradients near the pole edges as the three-dimensional do. Therefore the following results of POISSON are only a test for the success of the field correction using the shimming procedure described above.

As an example a half of a H-magnet with a pole piece which has the same size as the radius of the MAMI 3 magnet was calculated. From this field distribution the angle  $\beta$  of pole rotation was calculated according to eq. (2) in the middle of each mesh. The shims are then made by a polygon where the decrease between neighbouring mesh points is given by  $\beta$ .

Fig. 6 shows the field distribution in the mid-plane of the H-magnet without and with shims and the shape of the shims. The dotted line shows the ideal field calculated for infinite permeability, the dashed line the result for magnet iron.

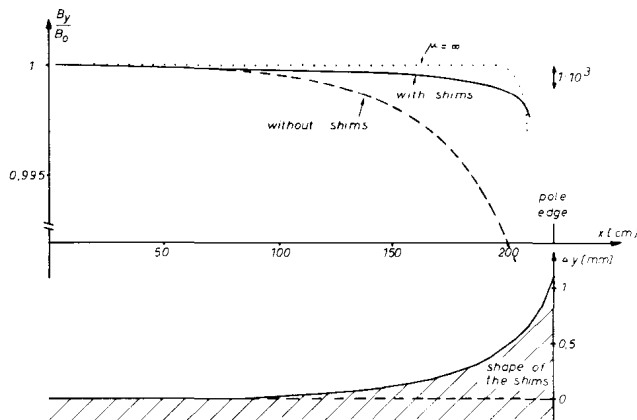


Fig. 6: Field distribution of a H-magnet with and without shims calculated by POISSON

The Geometry of the Reverse Field

Each end magnet of the third stage of MAMI will have a reverse field stripe<sup>8)</sup> in front of its pole edge in order to compensate the vertical defocusing of the fringe field. In opposition to the first and second stage of MAMI the active clamp is not fixed magnetically at the yoke.

Fig. 7 shows the geometry of the active and inactive clamp optimized by POISSON. The mirror plate in front of the upper (and lower) yoke is used to shield the stray flux. Its distance to the yoke is chosen in such a way that the flux density which is needed for vertical focusing in the reverse field is absorbed. The reverse field coils compensate the part of this flux which is closed through the inactive clamp. Therefore it has not to be closed magnetically. Because this equilibrium of flux is labile there are additional correction coils to produce flux in the mirror plate if the amplitude of the reverse field has to be changed within a small region.

The distance between the mirror plate and the yoke is strongly dependent from the magnetic characteristic of the iron used. Therefore it must be optimized at the accomplished magnet.

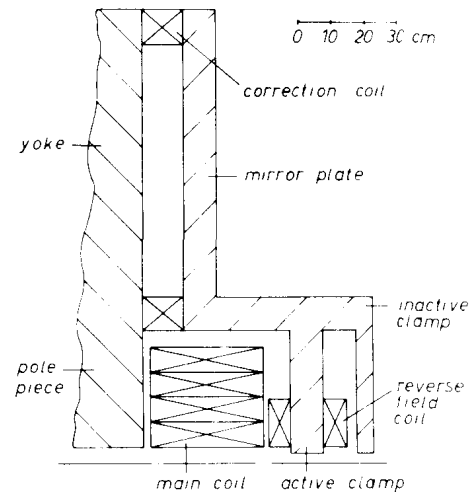


Fig. 7: Geometry of the reverse field of MAMI 3

Acknowledgements

We are gratefully obliged to W. Müller and his coworkers for doing the three-dimensional calculations with PROF1. B. Langenbeck's help for the use of the program POISSON is thankfully acknowledged. We appreciate further the opportunity to use the computers of GSI Darmstadt.

References

- 1) H. Herminghaus et al., Nucl Instr. & Meth. 138(1976) p. 1
- 2) H. Herminghaus, K.H. Kaiser, U. Ludwig, Nucl. Instr. & Meth. 187(1981) p. 103
- 3) H. Herminghaus et al., IEEE Transactions on Nuclear Science, Vol 30 No 4, Aug. 1983, p 3274
- 4) K.H. Kaiser, Internal Report MAMI 4/81, Institut für Kernphysik, Mainz
- 5) W. Müller et al., Archiv für Elektrotechnik 65(1982) p. 299
- 6) A.M. Winslow, Journal of Computational Physics 2, (1967) p. 149
- 7) R. Klein, U. Ludwig-Mertin, Internal Report MAMI 11/83, Institut für Kernphysik, Mainz
- 8) H. Babic, M. Sedlacek, Nucl. Instr. & Meth. 56(1967) p. 170